2-2-2010

A novel choline cotransporter sequestration compartment in cholinergic neurons revealed by selective endosomal ablation

Michael T. Ivy
Tennessee State University

Robert F. Newkirk
Tennessee State University

Yilun Wang
Meharry Medical College

James G. Townsel
Meharry Medical College

Recommended Citation

Ivy, M.T., Newkirk, R.F., Wang, Y. and Townsel, J.G. (2010), A novel choline cotransporter sequestration compartment in cholinergic neurons revealed by selective endosomal ablation. Journal of Neurochemistry, 112: 1295-1304. https://doi.org/10.1111/j.1471-4159.2009.06543.x

Journal of Neurochemistry

JOURNAL OF NEUROCHEMISTRY | 2010 | 112 | 1295–1304 doi: 10.1111/j.1471-4159.2009.06543.x

A novel choline cotransporter sequestration compartment in cholinergic neurons revealed by selective endosomal ablation

Michael T. Ivy,* Robert F. Newkirk,* Yilun Wang† and James G. Townsel†

*Department of Biological Sciences, Tennessee State University, Nashville, TN, USA

†Department of Neurobiology and Neurotoxicology, Meharry Medical College, Nashville, TN, USA

Abstract

The sodium-dependent, high affinity choline transporter – choline cotransporter – (ChCoT, aka: cho-1, CHT1, CHT) undergoes constitutive and regulated trafficking between the plasma membrane and cytoplasmic compartments. The pathways and regulatory mechanisms of this trafficking are not well understood. We report herein studies involving selective endosomal ablation to further our understanding of the trafficking of the ChCoT. Selective ablation of early sorting and recycling endosomes resulted in a decrease of ~75% of [^{3}H]choline uptake and ~70% of [^{3}H]hemicholinium-3 binding. Western blot analysis showed that ablation produced a similar decrease in ChCoTs in the plasma membrane subcellular fraction. The time frame for this loss was approximately 2 h which has been shown to be the constitutive cycling time for ChCoTs in this tissue. Ablation appears to be dependent on the intracellular cycling of transferrin-conjugated horseradish peroxidase and the selective deposition of transferrin-conjugated horseradish peroxidase in early endosomes, both sorting and recycling. Ablated brain slices retained their capacity to recruit via regulated trafficking ChCoTs to the plasma membrane. This recruitment of ChCoTs suggests that the recruitable compartment is distinct from the early endosomes. It will be necessary to do further studies to identify the novel sequestration compartment supportive of the ChCoT regulated trafficking.

Keywords: choline transport, compartmental ablation, recruitment, transporter trafficking.

J. Neurochem. (2010) **112**, 1295–1304.

The pre-synaptic high affinity choline transporter found at the cholinergic synapse has an obligatory requirement for the cotransport of sodium (Haga and Noda 1973; Yamamura and Snyder 1972; Simon *et al.* 1976),; thus, it is a symporter of choline and sodium (i.e. choline cotransporter, ChCoT aka: cho-1, CHT1, CHT; Okuda *et al.* 2000; Apparsundaram *et al.* 2000). Choline transporter activity has been shown to be rate-limiting in acetylcholine synthesis (Birks and MacIntosh 1961; Roskoski 1978; Newkirk *et al.* 1980). High frequency stimulation or its simulation with pre-exposure to depolarizing concentrations of potassium of cholinergic tissues results in a substantial increase in choline transport (Murrin and Kuhar 1976; Higgins and Neal 1982; Ferguson *et al.* 1994; Ford *et al.* 1999). Hemicholinium-3 (HC-3) binding studies in tissues have been used to confirm that the increase in transport is paralled by a comparable increase in the numbers of ChCoTs in the plasma membrane. In our laboratory the use of a plasmalemmal, impermeant, irreversible HC-3 mustard derivative demonstrated that the *Limulus* brain ChCoT trafficks constitutively into and out of the plasma membrane (Ivy *et al.* 2001). Cell-surface biotinylation and confocal microscopy were used in both SN56 and HEK293 cultured cell lines, to show that the choline cotransporter constitutively and rapidly internalized from the cell surface in clathrin-coated vesicles and was directed to early endosomes via a clathrin-dependent endocytic trafficking mechanism (Ribeiro *et al.* 2005). Moreover, recent studies by Ribeiro *et al.* (2007) provide evidence that the

Received September 3, 2009; revised manuscript received December 2, 2009; accepted December 7, 2009.

Address correspondence and reprint requests to James G. Townsel, Department of Neurobiology and Neurotoxicology, Meharry Medical College, 1005 D.B. Todd Blvd., Nashville, TN 37208, USA.
E-mail: jtownsel@mmc.edu

Abbreviations used: AnEK, antecedent elevated potassium; ChCoT, cho-1, CHT1, CHT, choline transporter; DAB, diaminobenzedine; ER, early recycling endosome; ES, early sorting endosome; FP, fusion peptide of ChCoT; GAT1, GABA transporter-1; GLUT4, glucose transporter-4; H_2O_2, hydrogen peroxide; HC-3, hemicholinium-3; HRP, horseradish peroxidase; IRAP, insulin-regulated aminopeptidase; LE, late endosome; Lys., lysosome; MM, microsomal membranes; PM, plasma membrane; Tf, transferrin; TfR, Tf receptor.

choline transporter recycles back to the plasma membrane both in a constitutive and a regulated mode.

The selective endosomal ablation strategy takes advantage of the known trafficking pattern of the transferrin receptor (TfR) through the early endosomal pathway (Mellman 1996). TfRs at the cell surface upon binding its target, Tf protein, undergoes endocytosis. The TfR-Tf complex traffics via the early sorting and early recycling (trafficking) endosomes back to the plasmalemma. Selective endosomal ablation is based on the specific accumulation of TfR-Tf-horseradish peroxidase (HRP) complex in the early endosomal pathway (Sheff *et al.* 2002). The selective endosomal ablation protocol has been used in the study of the insulin responsive glucose transporter (GLUT4) trafficking (Livingstone *et al.* 1996; Hashiramoto and James 2000). More recent studies have implicated a sequestration compartment within adipocytes for GLUT4 that survives TfR-Tf-HRP mediated endosomal ablation (Zeigerer *et al.* 2002; Karylowski *et al.* 2004). In the studies reported here, we evaluated the effect on the surface distribution of the ChCoTs following the application of the selective endosomal ablation protocol in *Limulus* brain hemi-slices. Ablated brain slices were used to examine indirectly, both constitutive and regulated trafficking of the ChCoT. Choline uptake measurements, HC-3 binding determinations and western blotting were performed to assess changes in choline uptake and the redistribution of the ChCoT.

Materials and methods

Animals and tissue preparation

Horseshoe crabs (*Limulus polyphemus*) of either sex were purchased from the Marine Biological Laboratory (Woods Hole, MA, USA), and were maintained in moist excelsior at 4–8°C until the time of use. Animals averaging 15–30 cm across the carapace were used in all experiments. The corpora pedunculata and protocerebrum complex were removed, placed in normal Chao's (440 mM NaCl, 9 mM KCl, 37 mM $CaCl_2$, 10 mM HEPES; pH 7.4) (Chao 1933), divided into hemispheres, mounted with Tissue Tek onto a Campden vibroslicer stage, and placed at −10 to −15°C for 5 min before slice preparation. Brain hemi-slices (500 μm thickness) were prepared using a vibroslicer, blotted, weighed and allowed to equilibrate in normal Chao's at 25°C prior to either choline transport or HC-3 binding experiments. Data points for all experiments were obtained in at least triplicate and statistical significance was assessed using a Student's *t*-test.

Compartmental ablation strategy

The TfR appears to be a ubiquitous integral membrane protein that has been shown to bind its ligand, Tf and the complex is rapidly endocytosed. This complex traffics via the early sorting (ES) endosome and the early recycling (ER) endosome compartments back to the plasma membrane (Hopkins and Trowbridge 1983; Presley *et al.* 1993; Mellman 1996). Notably, Sheff *et al.* (2002) have elucidated the detailed trafficking of the TfR using both intact and microsurgically manipulated cytoplasts. In these studies, they show that the primary trafficking of TfR back to the plasma membrane occurs directly from the ES endosome (74%), while a minor component (26%) travels from the ES endosome to the ER endosomal compartment enroute to the surface membrane. A unique aspect of either the TfR-Tf or the substituted TfR-Tf-HRP complex exploited in the endosomal ablation strategy is that the TfR-Tf-HRP complex remains intact until it resurfaces at the plasma membrane. At equilibrium both early endosomal compartments are saturated with the TfR-Tf complex (Sheff *et al.* 2002). The strategy for selective endosomal ablation relies upon the saturation of these compartments with TfR-Tf-HRP complex and the subsequent treatment with 3,3′-diaminobenzidine (DAB, 2 mg/mL, Vector Laboratories, Burlingame, CA, USA) and hydrogen peroxide (H_2O_2, 0.02%) in a buffer solution (Livingstone *et al.* 1996). As stated in the paper of Livingstone *et al.*, the technique cross-links and renders insoluble ('ablate') intracellular compartments containing the TfR by means of a Tf-HRP conjugate. The premise of the selective endosomal ablation strategy is presented in Fig. 1. In this study, selective endosomal ablation was achieved by an initial pre-incubation of brain hemi-slices in the presence Tf-HRP conjugate in normal Chao's solution for 30 min at 37°C. Following this 30 min incubation, 1 mL of ice-cold quenching buffer (sodium citrate in buffered Chao's) was added to each slice. The slices were aspirated and subsequently washed with several (1 mL) volumes of ice-cold buffered Chao's and then incubated in Chao's containing DAB plus H_2O_2 for 1 h in the dark at 4–8°C. Control slices were incubated in Chao's containing DAB without H_2O_2. Fig. 1(a) models the predicted trafficking pattern of the TfR-Tf-HRP complex and Fig. 1(b) models the consequence of the ablation of the ES endosome and ER endosome on subsequent trafficking involving these early endosomes.

Choline transport and hemicholinium-3 specific binding measurements

The brain hemi-slices were prepared as described above. The initial set of experiments were designed to measure [^{3}H]choline uptake for determination of the time course following completion of the 1 h ablation or control (DAB with no H_2O_2) treatment. After this treatment, the hemi-slices were washed in normal Chao's for different times (10, 30, 60, 90, 120 and 180 min) and transferred to microtubes containing either normal Chao's or normal Chao's + 200 μM HC-3 in the presence of 1 μM [^{3}H]choline (86.6 Ci/mmol; New England Nuclear, Newton, MA, USA) and incubated for 30 min at 25°C. Subsequently each slice was washed, solubilized and Polyfluor (Packard Instrument Company, Meriden, CT, USA) was added to determine the radioactive content by liquid scintillation spectrometry. Low affinity choline transport was defined as uptake observed in the presence of 200 μM HC-3. The post-ablation high affinity choline transport was calculated by subtracting the low affinity choline uptake from total choline uptake. Transport is expressed as picomoles of [^{3}H]choline per mg of tissue per unit time.

In experiments designed to assess HC-3 binding, following the 1 h ablation or control treatment, hemi-slices were washed with normal Chao's for either 10 or 120 min at 25°C. Next, the slices were incubated in normal Chao's containing either 10 nM [^{3}H]HC-3 (120 Ci/mmol) in the absence (total binding) or presence of 200 μM unlabeled HC-3 (non-specific binding) for 30 min at 25°C.

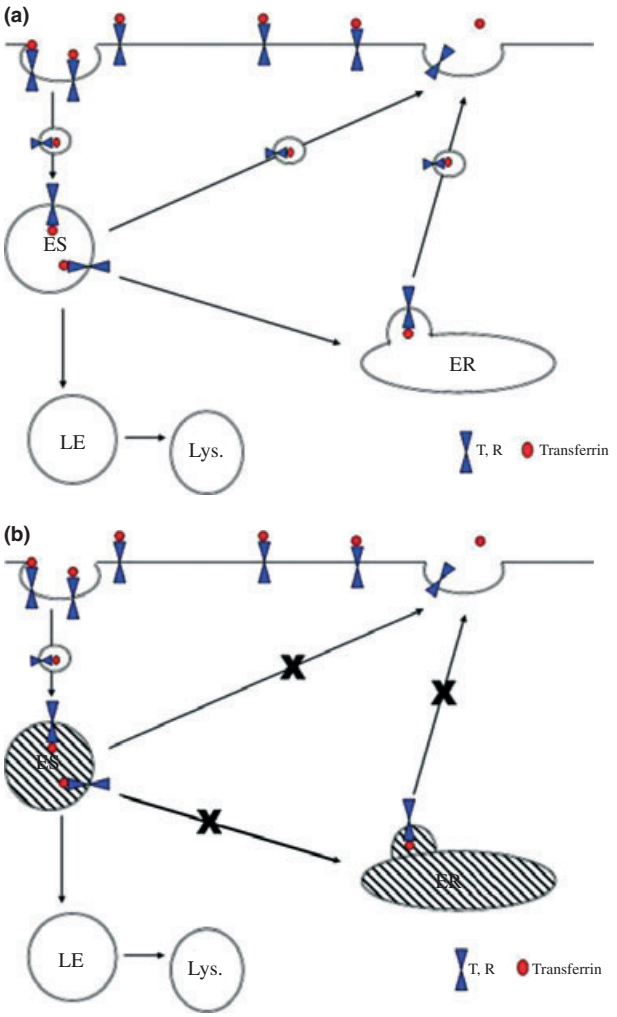

Fig. 1 Intracellular trafficking model for the transferrin receptor (TfR). (a) The TfR with bound Tf cycles via the early sorting (ES) endosome and the early recycling (ER) endosome back to the surface membrane. Additional endosomes are the late endosome (LE) and lysosome (Lys.). (b) Early endosomes are presumed saturated with the transferrin–horseradish peroxidase complex bound to the TfR. Treatment with diaminobenzedine plus hydrogen peroxide (H_2O_2) results in a chemical cross-linking rendering both endosomes non-functional (cross-hatching). Blockage of these endosomes is indicated by (X).

Incubations were terminated by rapidly washing the tissues with ice-cold normal Chao's and samples were prepared for liquid scintillation counting as described above. Specific binding was determined as the difference between total binding and non-specific binding. Post-ablation specific binding is expressed as femtomoles of [^{3}H]HC-3 bound per mg of tissue per unit time.

The recruitment of ChCoTs to the plasma membrane was achieved by the established protocol in which brain hemi-slices were subjected to antecedent exposure to depolarizing concentrations of potassium chloride [antecedent elevated potassium (AnEK)] in Chao's. Hemi-slices were pre-incubated in either normal Chao's (control) or 120 mM K^+ Chao's for 15 min at 25°C, washed in 2–5 minute exchanges in normal Chao's, before incubation with [^{3}H]choline. After washing slices were incubated in 1 μM [^{3}H]choline in normal Chao's for 30 min at 25°C. Subsequently, the radioactive content of each slice was measured as previously described. Uptake was calculated in pmoles/mg of tissue/30 min. HC-3 binding was assessed in either control or AnEK pre-treated slices washed in Chao's, and then incubated in [^{3}H]HC-3 (10 nM) in Chao's to determine the surface population of transporters. Specific binding was determined by assessing [^{3}H]HC-3 binding in the presence and absence of 200 mM unlabeled HC-3. Following normal Chao's washes, the radioactive content of each slice was determined by liquid scintillation spectrometry.

To determine whether or not the recruitable pool of ChCoTs resides within the set of early endosomes, the AnEK challenge and compartmental endosomal ablation were used. Measurement of [^{3}H]choline uptake and the determination of [^{3}H]HC-3 binding were assessed in both ablated brain hemi-slices and ablated slices challenged subsequently with AnEK. Compartmental ablation was achieved as previously described. Ablated hemi-slices were washed and incubated with either [^{3}H]choline or [^{3}H]HC-3. Choline uptake and HC-3 binding were measured as mentioned above. The effect of AnEK challenge on ablated slices was determined following a 2 h wash. Ablated and washed slices were incubated for 15 min in Chao's containing 120 mM KCl and subsequently placed in two 5 min washes of normal Chao's. In separate preparations of ablated and AnEK challenged hemi-slices, either [^{3}H]choline uptake or [^{3}H]HC-3 binding was measured. In a parallel set of experiments, these measurements were performed in hemi-slices subjected to both a pre-ablation AnEK challenge followed by a post-ablation challenge.

Subcellular fractionation

Limulus brain hemi-slices were subjected to a modified fractionation procedure (Simpson *et al.* 1983). Brain hemi-slices were homogenized in 20 mM Hepes, 250 mM sucrose buffer (pH 7.4) containing protease inhibitor cocktail (Sigma-Aldrich, St Louis, MO, USA) with a Dounce homogenizer using 12 up and down strokes on ice. The homogenate was subjected to a centrifugation of 940 *g* for 10 min at 4°C. The supernatant was then recentrifuged at 16 100 *g* for 15 min to produce crude plasma membrane (PM) and microsomal membrane (MM) fractions. From these fractions, proteins were extracted at 4–8°C for 1 h using 20 mM Hepes buffer containing 1% Triton X-100. All fractions were frozen quickly in isopentane and stored at −80°C until used.

Custom antibody for *Limulus* choline cotransporter

An antibody raised against the *Limulus* ChCoT was custom developed by Invitrogen Life Technologies Corporation (Zymed Laboratories, Carlsbad, CA, USA). The epitope used in raising the antibody consisted of an 18 amino acid (aa) sequence from the carboxyl-terminal (C-18) of the cloned *Limulus* ChCoT (Wang *et al.* 2001). The polyclonal antibody was raised in rabbit and was affinity purified. A fusion peptide (FP) was constructed as a positive control. The FP consisted of 77 aa from the C-terminal of the *Limulus* ChCoT. The recombinant peptide was expressed in pGEX-6P-1 vector (Amersham Pharmacia Biotech, Piscataway, NJ, USA), subcloned via restriction enzyme Bam *H1* and Not *1*. Purification was completed using Glutathione Sepharose 4B. Samples of the

Limulus ChCoT FP were dissolved in homogenate buffer and placed on isopentane for storage until further analysis. These samples were used as positive controls in assessing the specificity of the custom antibody. The primary antibody dilution was made by placing anti-ChCoT in a volume 1 : 5000 in SuperBlock Blocking Tris-buffered saline (Pierce) and maintained at 0–4°C until used. The pre-absorbed antibody dilution was made by combining equal volumes of anti-ChCoT and C-18 peptide at a ratio of 1 : 20, and shaking gently overnight at 0–4°C. One volume of the pre-absorbed anti-ChCoT was diluted at 1 : 2500 in SuperBlock and maintained at 0–4°C until used. Secondary antibody (goat anti-rabbit-IgG-HRP; Vector Laboratories, Inc.) dilution was 1 : 300 000 in SuperBlock and maintained at 0–4°C until used.

FP samples and protein extracts from *Limulus* brain tissues (PM and MM fractions) stored in the presence of protease inhibitor cocktail (Sigma-Aldrich), were separated by sodium dodecyl sulfate–polyacrylamide gel electrophoresis using 10% polyacrylamide pre-cast gels. Proteins were electrophoretically transferred to nitrocellulose membranes (0.22 μm; Osmonics Inc., Vista, CA, USA). The nitrocellulose membranes were blocked for 1 h in SuperBlock buffer. Antigens were detected by incubation of the membranes with diluted primary antibody or diluted pre-absorbed antibody. The membranes were incubated for 1 h with shaking at 25°C or at 4–8°C overnight. Membranes were subsequently placed in six 5 min washes of blocking buffer, following by incubation for 45 min in secondary antibody solution with gentle shaking at 25°C. After five washes with Tris-buffered saline, the immune complexes were visualized by chemiluminescence (Supersignal West Femto Maximum Sensitivity Substrate; Pierce, Rockford, IL, USA) using an UVP imaging system. To quantify the amount of ChCoT detected in the PM and MM fractions, the band densities were measured with the UVP imaging software for optical density determinations.

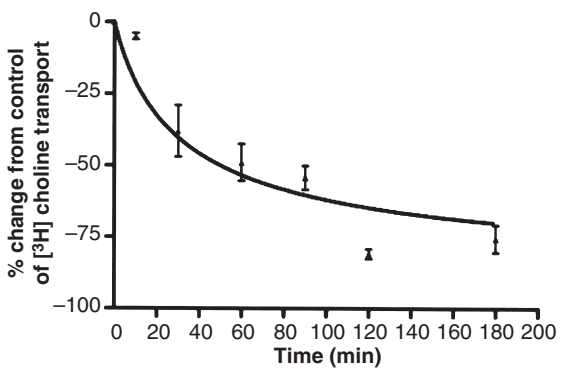

Fig. 2 Time course for loss of plasma membrane choline cotransporters after ablation. Brain hemi-slices were pre-treated with either transferrin–horseradish peroxidase conjugate or normal Chao's solution (control) for 30 min at 37°C, after which hemi-slices were treated with diaminobenzedine for 1 h at 4°C. Following treatment, hemi-slices were washed in normal Chao's for varying times from 0 to 180 min at 25°C and subsequently, slices were incubated in 1 μM [^{3}H]choline Chao's for 30 min at 25°C. Data are plotted as the difference between the ablated and control, and represent the mean ± SEM for at least 3 determinations.

Results

Time course for the loss of surface choline transporters following ablation

As previously presented, the selective endosomal compartment ablation strategy is predicated on disrupting the equilibrium between the exocytotic insertion and the endocytotic retrieval of ChCoTs in the plasma membrane. Thus, the expectation was that the reduction of surface transporters would be time-dependent. To determine the time course of the loss or retrieval of plasmalemmal ChCoTs following the ablation treatment, we examined the rate of [^{3}H]choline uptake at varying times following the ablation paradigm. The results are presented in Fig. 2. Surface transporters, as measured by changes in [^{3}H]choline uptake, declined exponentially with the maximal effect (~80% reduction) occurring at approximately 2 h post-ablation. This 2-h time course agrees well with the constitutive cycling time previously reported for the ChCoT (Ivy *et al.* 2001). To assess the possible immediate effect of the ablation protocol on the distribution of the surface transporters, we measured [^{3}H]HC-3 specific binding as well as [^{3}H]choline uptake at two time-points post-ablation, 10 and 120 min (Table 1). The results show that at 10 min, there were no measurable differences in [^{3}H]HC-3 binding nor [^{3}H]choline uptake between controls and tissues subjected to the ablation protocol. Conversely, at 2 h, there was a highly significant reduction in both HC-3 binding (67%) and choline uptake

Table 1 [^{3}H]Choline uptake and [^{3}H]hemicholinium-3 specific binding 10 and 120 min post-ablation

	[^{3}H]Choline uptake pmol/mg/30 min	[^{3}H]HC-3 specific binding fmol/mg/30 min
10 min wash		
Chao's (control)	1.19 ± 0.09	4.91 ± 0.56
Post-ablation	1.03 ± 0.05	4.51 ± 0.34
% Change	ND	ND
120 min wash		
Chao's (control)	0.95 ± 0.06	3.71 ± 0.43
Post-ablation	0.23 ± 0.09*	1.21 ± 0.05*
% Change	–75.8	–67.4

Brain hemi-slices pre-treated for 30 min with Tf-HRP, were exposed then to either DAB + H_2O_2 (ABLATION protocol) in normal Chao's or normal Chao's (Control) for 60 min at 4°C in the dark. Following this treatment, each hemi-slice was washed either 10 or 120 min in normal Chao's plus BSA (5 mg/mL). Subsequently, each slice was incubated in normal Chao's containing either 1 μM [^{3}H]Choline (86.6 Ci/mmol) or 10 nM [^{3}H]HC-3 (120 Ci/mmol) for 30 min at room temp. Data are the mean ± SEM for at least three determinations.

ND, no difference.

*$p < 0.05$, significantly different from Chao's (control) solution (Student's *t*-test).

(76%). These results show that the decrease in choline uptake in selective ablated brain hemi-slices is accompanied by a comparable reduction in the number of surface transporters. Moreover, these results are consistent with the constitutive cycling of ChCoTs as previously reported by this laboratory (Ivy *et al.* 2001).

The requirement of Tf conjugated with HRP for effective ablation

The selective compartmental ablation strategy relies upon the presence of the TfR which specifically transports Tf-HRP to the early endosomal compartments (Sheff *et al.* 2002). The *Limulus* TfR has not been cloned nor identified. Thus, a set of experiments were carried out to show the essential requirement of tranferrin conjugated with HRP, therefore implicating a TfR or a TfR-like protein in *Limulus* brain hemi-slices. Brain tissues were treated with various configurations with and without HRP-conjugated Tf. Additionally, DAB was applied with and without H_2O_2. The results seen in Fig. 3 demonstrate the unequivocal requirement for the Tf-HRP conjugate to achieve compartmental endosomal ablation. These findings suggest that the HRP conjugated to Tf is internalized and is accumulated selectively in the early endosomal compartments known to be involved in TfR trafficking back to the plasma membrane. Therefore, the chemical interaction between DAB and H_2O_2 with Tf-HRP aggregated selectively within the early endosomal compartments which results in the ablation of traffick through these cytosolic compartments (Sheff *et al.* 2002). Also, Sheff *et al.* used a kinetic analysis in determining that the TfR trafficks through both the ES endosomes and early trafficking (recycling) endosomes enroute back to the plasma membrane.

Choline transporter recruitment in brain hemi-slices confirmed by western blotting

It is well established that high frequency stimulation results in the doubling of choline transport in cholinergic neurons (Birks and MacIntosh 1961; Potter 1970). High frequency stimulation can be simulated by a paradigm of a brief exposure (~15 min) of nervous tissue to a depolarizing concentration of KCl followed by a 10 min wash, and a return of tissue to its normal physiologic bath. Following this treatment, choline uptake is doubled as are the number of ChCoTs in the plasma membrane. This experimental paradigm is referred to as the AnEK challenge.

To visualize the recruitment source of the ChCoT to the cell surface, we used western blot analysis of plasma and microsomal membrane extracts. The custom synthesized antibody was tested for specificity as described in the Materials and methods and the results are shown in Fig. 4. The ChCoT antibody recognized a protein of approximately 70 kDa in both PM and MM fractions. It also

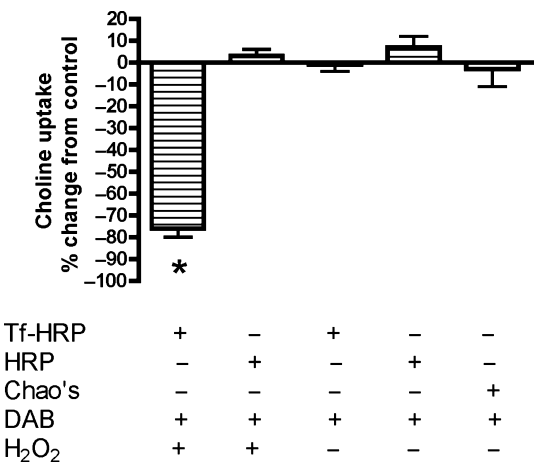

Fig. 3 The effects of horseradish peroxidase (HRP) conjugated transferrin (Tf) on high affinity choline transport. Brain hemi-slices were pre-treated with either Tf-HRP conjugate, unconjugated HRP, or normal Chao's solution (control) for 30 min at 37°C. After quenching and washing, hemi-slices were subjected separately to either diaminobenzedine (DAB) + H_2O_2, DAB or H_2O_2 for 1 h at 4°C. All slices were washed in normal Chao's for 120 min at 25°C, and subsequently, were incubated in 1 μM [^{3}H]choline Chao's for 30 min at 25°C. The data values are expressed as percentages of the control uptake shown as 0 on the *Y* axis. Data are the mean ± SEM for at least three determinations. *$p < 0.05$ versus control values (Student's *t*-test).

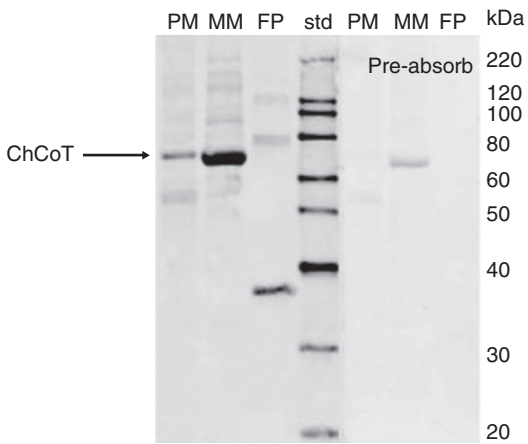

Fig. 4 Specificity of custom choline cotransporter antibody. Western blot analysis of choline cotransporter (ChCoT) expression in *Limulus* brain hemi-slice extracts of plasma membrane (PM) and microsomal membrane (MM) fractions were performed using a polyclonal ChCoT custom synthesized antibody. Immunoblotting of subcellular fraction protein extracts and samples of a fusion peptide (FP; positive control) was carried out. The ChCoT antibody identified a ~70 kDa band from both the PM and MM fractions, and showed a single band (~35 kDa) from the FP. The pre-absorbed control failed to identify the FP and ~70 kDa PM band; the ~70 kDa MM band was greatly reduced. Representative images from independent experiments ($n = 3$) are shown.

interacted with the positive control fusion peptide (FP, ~35 kDa). Pre-absorption of the antibody with the C-18 peptide blocked antibody interaction with the 70 kDa proteins in membrane extracts and also with the FP. These results confirm the specificity of the custom antibody. Furthermore, boiling the custom antibody for 10 min produced the same blockage of antibody interaction with the 70 kDa proteins in membrane extracts as well as the FP (data not shown).

We and others have shown that prior sustained depolarization of cholinergic nervous tissues lead to an increase of both the numbers of ChCoTs in the plasma membrane as well as a complementary enhancement of [^{3}H]choline uptake by these tissues (Roskoski 1978; Newkirk *et al.* 1980; Ribeiro *et al.* 2003). Antecedent elevated KCl Chao's exposure results in a doubling of [^{3}H]choline uptake compared to controls with a corresponding increase in [^{3}H]HC-3 binding as shown in Fig 5(a). Western blot analysis of PM and MM fractions confirm the increase in surface ChCoTs resulting from AnEK challenge (Fig. 5b). Others (Ferguson *et al.* 2003; Nakata *et al.* 2004) have shown and we confirm that the majority of the ChCoT distribution is intracellular. The apparent effect of the AnEK challenge is to redistribute the transporter from intracellular stores to the PM.

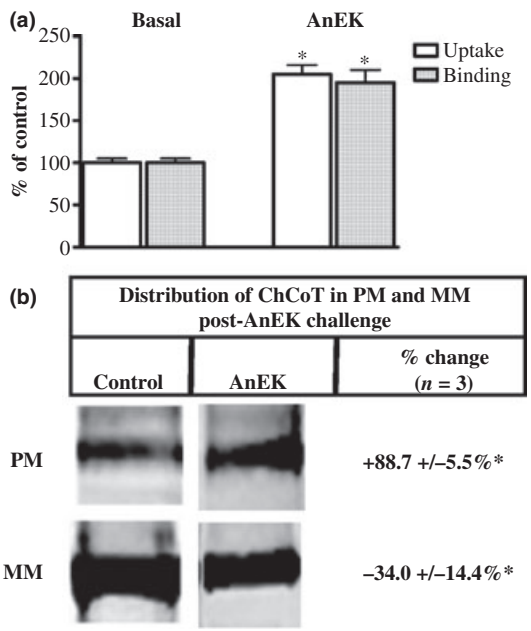

Fig. 5 The effects of antecedent elevated potassium on high affinity choline transport and hemicholinium-3 specific binding. Brain hemi-slices were subjected to separate 15 min pre-treatments in either normal Chao's (basal/control conditions) or 120 mM potassium (K^+) Chao's (antecedent elevated potassium, AnEK) solution at 25°C, and subsequently slices were used for (a) [^{3}H]choline uptake and [^{3}H]HC-3 binding measurements, or (b) ChCoT antibody western blot analysis. For uptake and binding (a), hemi-slices were incubated either in 1 μM [^{3}H]choline or 10 nM [^{3}H]HC-3 Chao's solution for 30 min at 25°C. Average control values for choline uptake 1.93 ± 0.71 pmol/mg tissue, and for HC-3 specific binding 6.43 ± 1.42 fmol/mg tissue. AnEK treatment caused a doubling of both choline uptake and HC-3 specific binding. Data are the mean ± SEM for at least three determinations. *$p < 0.05$ versus control values (Student's *t*-test). In western blots (b), the plasma membrane (PM) and microsomal membrane (MM) extracts showed a shift of ChCoTs to the PM, with a decrease from MM stores. Densities of PM and MM bands were measured and compared in calculating % changes. Data are the mean ± SEM with ($n = 3$) for each value; representative blots from separate experiments are shown.

The relationship of presumed early endosomal compartments to the recruitable compartment of choline transporters

Western blot analysis shows that the compartmental endosomal ablation treatment of *Limulus* brain hemi-slice preparations caused a significant decrease (~67%), in ChCoT levels in the PM fraction (Fig. 6). In an effort to assess the relationship of the ablated compartments with the recruitable population of ChCoTs, we subjected ablated tissues to an AnEK challenge. In tissues that were 2 h post-ablation, significant reductions in both [^{3}H]choline uptake (~80%) and [^{3}H]HC-3 binding (~75%) were observed (Fig. 7, column 1). The AnEK challenge of these two hour post-ablated tissues resulted in a full restoration of ChCoTs to the surface membranes as determined by [^{3}H]choline uptake and [^{3}H]HC-3 binding (Fig. 7, column 2). To further examine a possible relationship of the storage compartment responding to the AnEK challenge with the endosomal compartments, we altered the experimental protocol. In these experiments, the tissues were initially challenged with AnEK, ablated, and following a 2-h hold, subjected to a second AnEK challenge. These results are shown in Fig. 7, column 3. As can be seen in these results, the second AnEK challenge failed to restore the ablated preparations to their control or pre-ablated levels of either [^{3}H]choline uptake or [^{3}H]HC-3 binding. The

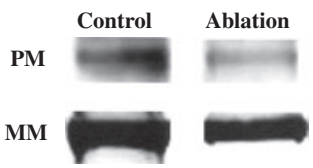

Fig. 6 The effect of ablation on the choline cotransporter subcellular distribution. Western blots shown for brain slices following either the control (no ablation) or ablation protocol in which tissues were treated with only diaminobenzedine or diaminobenzedine + H_2O_2 for 1 h at 4°C, respectively. Subsequently, slices were homogenized and subcellular fractionated into plasma membrane (PM) and microsomal membrane (MM) samples. PM and MM extracts were used in sodium dodecyl sulfate–polyacrylamide gel electrophoresis. Densities of PM and MM bands of several experiments ($n = 3$) were used in determining the relative intensities before and after ablation. Results show a loss of ChCoTs from the PM following ablation. *$p < 0.05$ versus control values (Student's *t*-test).

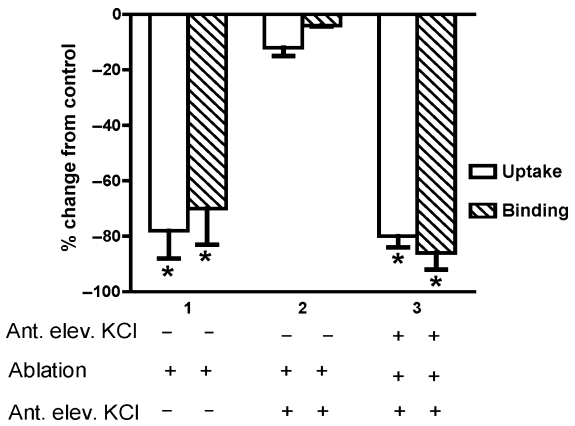

Fig. 7 The effect of antecedent elevated potassium challenge on choline cotransport and hemicholinium-3 specific binding in ablated *Limulus* brain hemi-slices. First, brain hemi-slices were incubated with the Tf-HRP for 30 min at 37°C followed by DAB cytochemistry for 1 h at 4°C. Subsequent to ablation and normal Chao's washes for 120 min at 25°C, slices were incubated in Chao's containing either 1 μM [^{3}H]choline or 10 nM [^{3}H]HC-3 for 30 min at 25°C and results are shown in lane 1. The 0 across the top of the graph represents control values for both uptake and binding determinations. Second, brain tissues were subjected to ablation, normal Chao's washes and antecedent elevated KCl treatment prior to being incubated with either 1 μM [^{3}H]choline or 10 nM [^{3}H]HC-3 for 30 min with the findings shown (lane 2). Third, hemi-slices were initially exposed to antecedent elevated KCl, ablated, and then treated with a second antecedent elevated KCl challenge after which [^{3}H]choline uptake or [^{3}H]HC-3 binding were measured. Results are shown in lane 3, and are the means ± SEM with n = 3–5 for each value. Results significantly differ from normal Chao's treatment *$p < 0.05$ (Student's t-test).

apparent failure of a second AnEK challenge to recruit ChCoTs to the surface membrane could be explained by the presence of a sequestration compartment specific for the recruitable population of ChCoTs with limited storage capability, and thus requiring a kinetic link to early endosomes for replenishment.

Discussion

Previously, the paradigm employing Tf conjugated with HRP and DAB plus H_2O_2 cytochemistry to produce selective endosomal compartmental ablation has been used in studies of the trafficking of the insulin responsive GLUT4 transporter (Livingstone *et al.* 1996; Hashiramoto and James 2000; Sheff *et al.* 2002; Zeigerer *et al.* 2002). In the studies reported herein, we have employed this selective endosomal ablation strategy to assess ChCoT trafficking in *Limulus* brain hemi-slices. As depicted in Fig. 1, the experimental strategy is predicated on the deposition of Tf-HRP in selective endosomal compartments resulting from the established intracellular trafficking of the TfR upon binding its natural ligand Tf. The Tf-HRP mediated ablation protocol applied to *Limulus* brain slices resulted in a maximal reduction (~80%) in [^{3}H]choline uptake at 2 h post-ablation (Fig. 2). Furthermore, the results presented in Table 1 demonstrate that the endosomal ablation protocol has no immediate effect on the surface population of ChCoTs. The TfR family of proteins appears to be rather ubiquitious, having been found extensively in both vertebrates and invertebrates (Lambert *et al.* 2005; Lambert and Mitchell 2007). The TfR has not been cloned or identified in *Limulus*. The experimental protocol used to generate the data summarized in Fig. 3 was designed to assess the strict requirement of HRP conjugated to the Tf protein to yield results reflective of selective endosomal ablation. The data presented in Fig. 3 clearly establish the essential requirement of HRP-conjugated Tf to achieve selective compartmental ablation as determined by cellular uptake of [^{3}H]choline in *Limulus* brain slices. These results argue strongly for the presence of a TfR or a Tf-like receptor protein in *Limulus*, and thus validate the use of this selective endosomal ablation paradigm in this preparation.

Numerous laboratories have confirmed an activity driven doubling of the transporter numbers in terminal membranes of cholinergic neurons (Mulder *et al.* 1974; Murrin and Kuhar 1976; Roskoski 1978; Newkirk *et al.* 1980; Higgins and Neal 1982). High frequency stimulation can be simulated by antecedent exposure of cholinergic nerves to depolarizing concentrations of KCl (AnEK), and produces the same effects. To aid in the resolution of the source of the ChCoTs recruited to the PM, we employed a custom antibody for the *Limulus* ChCoT in western blots of cellular membranes. The specificity of the antibody as resolved by antibody pre-absorption and is shown in Fig. 4. The results shown in Fig. 5(a) confirm the doubling of transport activity following AnEK. These results reflecting the doubling of transport activity agrees well with both the change in [^{3}H]HC-3 binding activity (~90%; Fig. 5a), and the changes in the relative optical density measurements in the western blots (~89%; Fig. 5b). Moreover, the data presented in Fig. 5(b) confirm that the increase in the plasmalemmal distribution of the ChCoTs results from the redistribution of these transporters from a cytoplasmic population of membranes (i.e. microsomal membranes) to the PM fraction. Western blot analyses of ablated preparations reveal a 67% decrease in the PM distribution of ChCoTs (Fig. 6). These results agree well with the reductions in specific [^{3}H]HC-3 binding as shown in Fig. 7, column 1. The reduction in the transporter distribution in the PM following selective compartment ablation is consistent with the view that these ChCoTs are continuously trafficking from the PM via cytoplasmic compartments back to the PM. The ablation strategy targets early endosomal compartments, and thus the selective loss of these compartments would agree with the results depicted in Figs 6 and 7, column 1. On

the other hand, the results summarized in Fig. 7, column 2, demonstrate that in ablated tissues in which the presumed early endosomes, central to continuous constitutive trafficking, are rendered non-functional, ChCoTs are recruitable from a yet to be described compartment. In a variation of the initial experimental paradigm in which an AnEK challenge preceded compartmental ablation treatment, a second AnEK challenge following ablation failed to recruit ChCoTs to the PM (Fig. 7, column 3). The results presented in Fig. 7, column 3, suggest a kinetic relationship between the endosomal compartments and the special compartment that houses the recruitable population of ChCoTs. (Ribeiro *et al.* (2003, 2005) used confocal microscopic observations of a choline transporter-hemagglutinin to show that the complex trafficks from the PM to endocytic organelles). Our laboratory employed an irreversible ligand of the ChCoT, a mustard derivative of HC-3, to show that ChCoTs constitutively traffics from the PM and back in approximately two hours (Ivy *et al.* 2001). The recruitment of the ChCoT with high frequency stimulation (using AnEK challenge) represents the regulated trafficking of the transporter. The results summarized in Fig. 7, are indicative of separate pathways serving the dual trafficking of ChCoTs, a pathway for constitutive trafficking that appears to involve early endosomes, and a regulated trafficking pathway that is primarily distinct from the early endosomes.

The observation that high frequency stimulation or antecedent depolarization with elevated potassium results in the recruitment of choline transporters to the PM has led to various speculations as to the underlying mechanism. One view expressed to explain high frequency stimulation and/or the AnEK challenge recruitment of choline transporters to surface membranes is that the transporter resides in synaptic vesicles. High frequency stimulation or antecedent exposure of cholinergic tissue to depolarizing concentrations of KCl would cause the increased release of neurotransmitter resulting from an increased fusion of synaptic vesicles with the terminal membrane. Concomitantly, the increased fusion of synaptic vesicles with the terminal membrane would also result in the deposition of transporter proteins into the plasma membrane (Ferguson *et al.* 2003; Ribeiro *et al.* 2003, 2006). Several studies have been reported that suggests that the choline transporter traffics in synaptic vesicles (Ferguson *et al.* 2003; Ribeiro *et al.* 2003; Nakata *et al.* 2004). On the other hand, there are reports that argue for caution in the interpretation of morphological evidence that all vesicles at the pre-synaptic terminal fit the classical definition of synaptic vesicles (i.e. vesicles containing neurotransmitter molecules). In studies of the plasma membrane-associated GABA transporter (GAT1), Deken *et al.* (2003), isolated the trafficking vesicle containing GAT1, and showed that these vesicles had the physical appearance of synaptic vesicles, and contained several proteins common to synaptic vesicles. However, these vesicles were not synaptic vesicles and did not contain synaptophysin, a protein common to synaptic vesicles. Neither did these vesicles contain GABA, the neurotransmitter associated with GAT1. These authors concluded that GAT1 resides in a vesicle morphologically similar to neurotransmitter-filled vesicles; however, they are not the classical synaptic vesicles, but rather synaptic-like vesicles.

The insulin responsive GLUT4 transporter is agruably the most extensively studied membrane transporter. The ChCoT has been shown to be a member of the sodium-dependent glucose transporter family and thus related to GLUT4 (Wang *et al.* 2001). Selective endosomal ablation experiments were used in the study of the trafficking of the GLUT4 (Livingstone *et al.* 1996). Results revealed two GLUT4 intracellular compartments, one is TfR positive and one is devoid of TfR. From these studies, it was concluded that the sequestration compartment surviving ablation is distinct from early endosomes. Bogan *et al.* (2003) published evidence for a non-endosomal cytoplasmic tethering mechanism involving a protein they termed tethering for the ubiquitin domain of

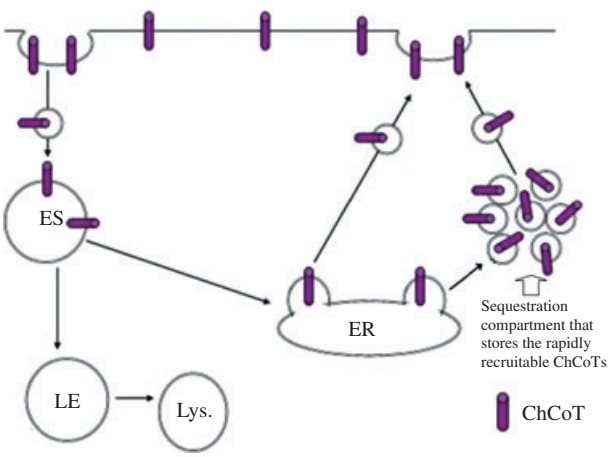

Fig. 8 Model for the dual (constitutive and regulated) trafficking of the choline cotransporter. The model depicts pathways through which the choline cotransporter (ChCoT) may traffic from and back to the cell surface. In the basal state, endocytosis of ChCoT vesicles fuse with early endosomes in close proximity to the plasma membrane (PM), thus removing transporters from the cell surface. The continuous constitutive trafficking of the ChCoTs appears to be from the PM to early endosomes, then back to the PM. High neuronal activity (simulated by antecedent exposure to depolarizing concentrations of KCl) triggers a rapid increase in the rate of exocytotic insertion of ChCoTs into the PM. A special sequestration compartment, distinct from early endosomes, appears to be the primary storage site of ChCoTs that are rapidly recruited to the PM (i.e. regulated trafficking). This specialized compartment, separate from early endosomes, does appear to require functioning endosomes for its replenishment. The results summarized herein, can be explained by the model in this figure.

the GLUT4. Our results are consistent with a model in which a 'specialized' sequestration compartment, containing the activity driven pool of ChCoTs, survives the ablation protocol (Fig. 8). The results that the pre-ablation AnEK challenge prevents a post-ablation AnEK challenge from restoring the *Limulus* brain slices to the pre-ablation levels suggests that the 'specialized' compartment for the ChCoT has a limited capacity, and requires intact, functional early endosomes for replenishment. In conclusion, we report that a storage/recruitment ChCoT pool persists following compartmental endosomal ablation driven by the early endosomal trafficking of the TfR-Tf-HRP complex. This result implies that a special compartment different from the classical early endosomes exists in cholinergic neurons and may be responsible for the sequestration of the activity driven ChCoTs. This population of transporters is required for adjusting cholinergic neuron output to meet activity driven demands. It is interesting to speculate on the status of this essential compartment in pathological states. Additional studies will be required to determine the physiological properties as well as the cellular location and structural nature of this compartment.

Acknowledgements

The authors thank Dr Purnima Ghose for technical assistance. Mrs Carolyn Davis and Mr Reginald Cannon for manuscript preparation. Also, we thank Drs Brenda S. McAdory and Sanika Chirwa for useful comments. This work was supported by NIH grants RR03032, MH57067 and P20MD000261.

References

Apparsundaram S., Ferguson S. M., George A. L. Jr and Blakely R. D. (2000) Molecular cloning of a human hemicholinium-3-sensitive choline transporter. *Biochem. Biophys. Res. Commun.* **276**(3), 862–867.

Birks R. and MacIntosh F. C. (1961) Acetylcholine metabolism of a sympathetic ganglion. *J. Biochem. Physiol.* **39**, 787–827.

Bogan J. S., Hendon N., McKee A. E., Tsao T. and Lodish H. F. (2003) Functional cloning of TUG as a regulator of GLUT4 glucose transporter trafficking. *Nature* **425**, 727–733.

Chao I. (1933) Action of electrolytes on the dorsal median nerve cord of the *Limulus* heart. *Biol. Bull. Mar. Biol. Lab. Woods Hole* **64**, 358–381.

Deken S. L., Wang D. and Quick M. W. (2003) Plasma membrane GABA transporters reside on distinct vesicles and undergo rapid regulated recycling. *J. Neurosci.* **23**, 1563–1568.

Ferguson S. S. G., Rylett R. J. and Collier B. (1994) Regulation of rat brain synaptosomal [^{3}H]hemicholinium-3 binding and [^{3}H]choline transport sites following exposure to choline mustard aziridinium ion. *J. Neurochem.* **63**, 1328–1337.

Ferguson S. M., Savchenko V., Apparsundaram S., Zwick M., Wright J., Heilman C. J., Yi H., Levey A. I. and Blakely R. D. (2003) Vesicular localization and activity-dependent trafficking of presynaptic choline transporters. *J. Neurosci.* **23**(30), 9697–9709.

Ford B. D., Ivy M. T., Mtshali C. P. and Townsel J. G. (1999) The involvement of protein kinase C in the regulation of choline cotransport in *Limulus*. *Comp. Biochem. Physiol.* **123A**, 255–261.

Haga T. and Noda H. (1973) Choline uptake systems of rat brain synaptosomes. *Biochim. Biophys. Acta* **291**, 564–575.

Hashiramoto M. and James D. E. (2000) Characterization of insulin-responsive GLUT4 storage vesicles isolated from 3T3-L1 adipocytes. *Mol. Cell. Biol.* **20**, 416–427.

Higgins A. J. and Neal M. J. (1982) Potassium activation of [^{3}H]choline accumulation by isolated sympathetic ganglia of the rat. *Br. J. Pharmacol.* **77**, 573–580.

Hopkins C. R. and Trowbridge I. S. (1983) Internalization and processing of transferrin and the transferrin receptor in human carcinoma A431 cells. *J. Cell Biol.* **97**, 508–521.

Ivy M. T., Newkirk R. F., Karim M. R., Mtshali C. M. P. and Townsel J. G. (2001) Hemicholinium-3 mustard reveals two populations of cycling choline cotransporters in *Limulus*. *Neurosci.* **102**, 969–978.

Karylowski O., Zeigerer A., Cohen A. and McGraw T. E. (2004) GLUT4 is retained by an intracellular cycle of vesicle formation and fusion with endosomes. *Mol. Biol. Cell* **15**, 870–882.

Lambert L. A. and Mitchell S. L. (2007) Molecular evolution of the transferrin receptor/glutamate carboxypeptidase II family. *J. Mol. Evol.* **64**, 113–128.

Lambert L. A., Perri H., Halbrooks P. J. and Mason A. B. (2005) Evolution of the transferrin family: conservation of residues associated with iron and anion binding. *Comp. Biochem. Physiol. B* **142**, 129–141.

Livingstone C., James D. E., Rice J. E., Hanpeter D. and Gould G. W. (1996) Compartment ablation analysis of the insulin-responsive glucose transporter (GLUT4) in 3T3-L1 adipocytes. *Biochem. J.* **315**, 487–495.

Mellman I. (1996) Endocytosis and molecular sorting. *Ann. Rev. Cell Dev. Biol.* **12**, 575–625.

Mulder A. H., Yamamura H. I., Kuhar M. J. and Snyder S. H. (1974) Release of acetylcholine from hippocampal slices by depolarization: dependence on high affinity choline uptake. *Brain Res.* **70**, 372–376.

Murrin L. C. and Kuhar M. J. (1976) Activation of high-affinity choline uptake *in vitro* by depolarizing agents. *Mol. Pharmacol.* **12**, 1082–1090.

Nakata K., Okuda T. and Misawa H. (2004) Ultrastructural localization of high-affinity choline transporter in the rat neuromuscular junction: enrichment on synaptic vesicles. *Synapse* **53**, 53–56.

Newkirk R. F., Maleque M. A. and Townsel J. G. (1980) Choline uptake, acetylcholine synthesis and release by *Limulus* abdominal ganglia. *Neurosci.* **5**, 303–311.

Okuda T., Haga T., Kanai Y., Endou H., Ishihara T. and Katsura I. (2000) Identification and characterization of the high-affinity choline transporter. *Nature Neurosci.* **3**, 120–125.

Potter L. T. (1970) Synthesis, storage and release of [^{14}C]acetylcholine in isolated rat diaphragm muscles. *J. Physiol.* **206**, 145–166.

Presley J. F., Mayor S., Dunn K. W., Johnson L. S., McGraw T. E. and Maxfield F. R. (1993) The *end2* mutation in CHO cels slows the exit of transferrin receptors from the recycling compartment but bulk membrane recycling is unaffected. *J. Cell Biol.* **122**, 1231–1241.

Ribeiro F. M., Alves-Silva J., Volknandt W. *et al.* (2003) The hemicholinium-3 sensitive high affinity choline transporter is internalized by clathrin-mediated endocytosis and is present in endosomes and synaptic vesicles. *J. Neurochem.* **87**, 136–146.

Ribeiro F. M., Black S. A. G., Cregan S. P., Prado V. F., Prado M. A. M., Rylett R. J. and Ferguson S. S. G. (2005) Constitutive high-affinity choline transporter endocytosis is determined by a carboxyl-terminal tail dileucine motif. *J. Neurochem.* **94**, 86–96.

Ribeiro F. M., Black S. A. G., Prado V. F., Rylett R. J., Ferguson S. S. G. and Prado M. A. M., (2006) The "ins" and "outs" of the high affinity choline transporter CHT1. *J. Neurochem.* **97**, 1–12.

Ribeiro F. M., Pinthong M., Black S. A. G., Gordon A. C., Prado V. F., Prado M. A. M., Rylett R. J. and Ferguson S. S. G. (2007) Regulated recycling and plasma membrane recruitment of the high-affinity choline transporter. *Eur. J. Neurosci.* **26**, 3437–3448.

Roskoski R. (1978) Acceleration of choline uptake after depolarization induced acetylcholine release in rat cortical synaptosomes. *J. Neurochem.* **30**, 1357–1361.

Sheff D., Pelletier L., O'Connell C. B., Warren G. and Mellman I. (2002) Transferrin receptor recycling in the absence of perinuclear recycling endosomes. *J. Cell Biol.* **156**, 797–804.

Simon J. R., Atweh S. and Kuhar M. J. (1976) Sodium-dependent high affinity choline uptake: a regulatory steip in the synthesis of acetylcholine. *J. Neurochem.* **26**, 909–922.

Simpson I. A., Yver D. R., Hissin P. J., Wardzala L. J., Karnieli E., Salans L. B. and Cushman S. W. (1983) Insulin-stimulated translocation of glucose transporters in isolated rat adipose cells: characterization of subcellular fractions. *Biochim. Biophys. Acta* **763**, 393–407.

Wang Y., Newkirk R. F., Ivy M. T. and Townsel J. G. (2001) Molecular cloning of a cDNA for a putative choline co-transporter from *Limulus CNS*. *Gene* **268**, 123–131.

Yamamura H. I. and Snyder S. H. (1972) Choline high-affinity uptake by rat brain synaptosomes. *Science* **61**, 626–628.

Yamamura H. I. and Snyder S. H. (1973) High affinity transport of choline into synaptosomes of rat brain. *J. Neurochem.* **21**, 1355–1374.

Zeigerer A., Lampson M. A., Karylowski O., Sabatini D. D., Adesnik M., Ren M. and McGraw T. E. (2002) GLUT4 retention in adipocytes requires two intracellular insulin-regulated transport steps. *Mol. Biol. Cell* **13**, 2421–2435.

